

Materials Research **Express**

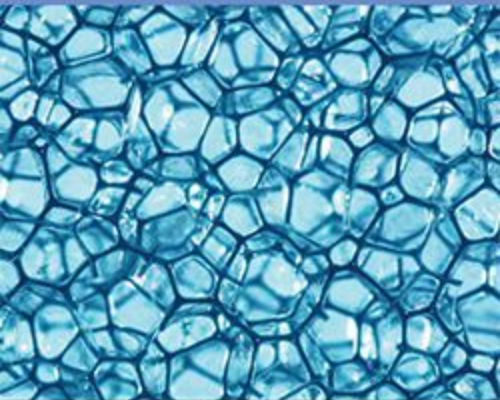


Table of contents

Volume 4
Number 3, March 2017
Previous issue Next issue

Buy this issue in print
Open all abstracts

Focus Papers

- Electronic structure of strongly correlated materials: from one-particle to many-body theory 034001
Structural, electronic and optical properties of Bi2O3 polymorphs by first-principles calculations for photocatalytic water splitting 034002
Synthesis and characterization of carbon nanotube/PVA/chitosan for security ink applications 034003
Effect of copper film catalyst substrate thickness on atomic diffusion time at the initiation of the recrystallization stage: a molecular dynamics study 034004
Composited reduced graphene oxide into LiFePO4/Li2SiO3 and its electrochemical impedance spectroscopy 034005
Microstructure and erosion study of porous Mg-Zn-Ca alloy in simulated body fluid 034006

Papers

- Nanomaterials and nanostructures
Carbon nanotube based hybrid nanocarbon foam 035001
Transmission in graphene through time periodic double barrier potential 035002
Self-organized growth of germanium nanocolumns 035003
Synthesis of indium selenide (In2Se3) by prior mechanical pulverization and mechanical alloying for thermoelectric applications 035004
Preparation of Cu-Fe-Al-O nanosheets and their catalytic application in methanol steam reforming for hydrogen production 035005
Optical, morphological, and electrical properties of P3HT: SiNWs nanocomposite deposited on flexible substrate: effect of SiNWs concentration 035007
Synthesis of graphene sheets from single walled carbon nanohorns: novel conversion from cone to sheet morphology 035008
Preparation of silver nanoparticles by using the hydrolyzates of poly(lactic acid) and their application for the antibacterial functionalization of poly(lactic acid) non-woven fabric 035009
Simple mass production of zinc oxide nanostructures via low-temperature hydrothermal synthesis 035010
Effect of temperature gradient on zinc oxide nano particles synthesized at low reaction temperatures 035011
Synthesis of SnO2(WO3)x nanocrystals via a statistically optimized route and their photocatalytic behavior 035012
Magnetic, specific heat and electrical transport properties of oxygen-deficient nanosized rutile TiO2-x 035013
Synthesis mechanism of sono-chemically prepared mesoporous ZnS nanoparticles 035014
Multiband (one hundred kilohertz) meta-atoms of microwave frequency 035015
An efficient photanode for dye sensitized solar cells using naturally derived S/TiO2 nanoparticles 035016
InN/InGaN dot-in-a-wire nanostructures emitting at 1.55 μm 035017
Tailoring luminescence properties of a sol-gel driven TiO2 nanoparticles by ammonia treatment 035018
The crack growth and expansion characteristics of Fe and Ni using quasi-continuum method 035019
Incorporation of coconut shell based nanoparticles in kenaf/coconut fibres reinforced vinyl ester composites 035020
New insights on the magnetic properties of ferromagnetic FePd3 single-crystals encapsulated inside carbon nanomaterials 035021
Effect of size and composition on the second harmonic generation from lithium niobate powders at different excitation wavelengths 035022
Sol concentration effect on ZnO nanofibers photocatalytic activity synthesized by sol-gel dip coating method 035023
Thermo-simulated evolution of crystalline structure and dopant distribution in Cu-doped Y-stabilized ZrO2 nanoparticles 035024
Magnetization and anomalous Hall effect in SiO2/Fe/SiO2 trilayers 035025
Graphene oxide modification of plexicon James in the strong coupling limit 035026
2D nano-Y2O3Eu3+ photoluminescence with different preparation methods and annealing temperatures 035027
Fabrication and evaluation of XF-1 loaded galactosylated chitosan nanoparticles for liver targeting 035028
Biosynthesis of spherical and highly stable gold nanoparticles using Fenalago Angulata aqueous extract: dual role of extract 035029
Zn1-xGd5x (x = 0.1, 0.2 and 0.3) nanoparticles for magnetic resonance imaging and optical fluorescence imaging 035030
Controllable synthesis of iron oxide nanoparticles in porous NaCl matrix 035031
Microfabrication with smooth thin carbon nanotube composite sheets 035032
Effective surface modification by chemical solution deposition for flexible metal substrates 035033
A first principle study on oxygen adsorption and incorporation on the (100) surface of [0 0 1]-oriented GaN nanowires 035034
Effect of particle size on gamma radiation shielding property of gadolinium oxide dispersed epoxy resin matrix composite 035035
Laser-induced fabrication of gold nanoparticles on shellac-driven peptide nanostructures 035036
Morphology and anisotropy of thin conductive inkjet printed lines of single-walled carbon nanotubes 035037
Highly photocatalytic activity of novel Fe-MIL-88B/GO nanocomposite in the degradation of reactive dye from aqueous solution 035038
α-Bi2O3 nanorods: synthesis, characterization and UV-photocatalytic activity 035039
Rapid synthesis of high purity gold nanorods via microwave irradiation 035040

Glasses and amorphous materials

- Energy efficiency of iron-boron-silicon metallic glasses in sulfuric acid solutions 036001
Network structure of SiO2 and MgSiO3 in amorphous and liquid States 036002
Electrical properties of Ge2S3 and Ge2S3-SnS4 glasses 036003
Effect of Li2O addition on structural and electrical properties of sodium borosilicate glasses 036004
Polymers
Effects of short glass fibers on the mechanical properties of glass fiber fabric/PVC composites 036001
Multi-objective optimization in the development of oil and water repellent cellulose fabric based on response surface methodology and the desirability function 036002
Mechanical behaviour of glass fibre reinforced composite at varying strain rates 036003
PMMA/PS coaxial electrospinning: core-shell fiber morphology as a function of material parameters 036004
Magnesium phenylphosphonate: a additive for poly(L-lactic acid) 036005
A capacitive sensor for 2,4-D determination in water based on 2,4-D imprinted polypyrrole coated pencil electrode 036006
Interaction of surfactants with block-copolymer systems in the presence of Hofmeister anions 036007

Energy and environment materials

- Polyaniline silver nanoparticle coffee waste extracted porous graphene oxide nanocomposite structures as novel electrode material for electrochemical capacitors 036001
Polyacrylic acid grafted kaolinite via a facile 'grafting to' approach based on heterogeneous esterification and its adsorption for Cu2+ 036002
Microstructure characterization of onion (A.capsa) peels and thin films for dye sensitized solar cells 036003
CO2 adsorption properties of ion-exchanged zeolite Y prepared from natural clays 036004
Nanogel-like grafted kaolinite via a facile 'grafting to' approach based on heterogeneous esterification and its adsorption for Cu2+ 036002
Microstructure characterization of onion (A.capsa) peels and thin films for dye sensitized solar cells 036003
CO2 adsorption properties of ion-exchanged zeolite Y prepared from natural clays 036004

Carbon materials

- Magneto-conductive encryption assisted by third-order nonlinear optical effects in carbon/metal nanohybrids 036001
Green synthesis of well-dispersed single-layer graphene colloids via an electrolytic method 036002
A facile one-step process for 3D N-doped noncovalent functionalization PS/GO composites 036003
Investigating the synergistic impedance match and attenuation effect of Co@C composite through adjusting the permittivity and permeability 036004
Flexible, thin films of graphene-polymer composites for EMI shielding 036005
Smart materials
Polyaniline silver nanoparticle coffee waste extracted porous graphene oxide nanocomposite structures as novel electrode material for electrochemical capacitors 036001
Grain size effect on mechanical performance of nanostructured superelastic NiTi alloy 036002
Thermoelectric properties of iso-electronically substituted bismuth compounds: a computational study 036003

Semiconductors

- First principle study of structural stability, electronic structure and optical properties of Ga doped ZnO with different concentrations 036001
Enhanced photo catalytic performance of nickel doped bismuth selenide under visible light irradiation 036002
Interactions between Er dopant and intrinsic point defects of ZnO: a first-principles study 036003
Reciprocal space mapping study of CdTe epilayer grown by molecular beam epitaxy on (110) 2B GaAs substrate 036004
Growth of freestanding lead dihalide thin films and microtubule via hydrothermal method 036005
Studies on structural, optical and magnetic properties of cobalt substituted magnetite fluids (CoFe2-xFe2O4) 036006
Study of Cu/Ni adsorption on GaN (100) D surface 036007
The effects of local bond relaxations on the electronic and photocatalytic performances of nonmetal doped 3R-MoO3 based photocatalytic density functional theory 036008
Positron annihilation spectroscopic characterization of defects in wide band gap oxide semiconductors 036009

Superconductors

- Effects of GaPz1/2Te1-xO3 polarization on the YBa2Cu3O7-x electrical transport and magnetization 036001
Magnetic materials
Estimates of the magnetoacoustic effect in (Ni,Cu)Mn2O3 and (Gd,Ca)MnO3 based on magnetic transition entropies 036001
Magnetism in the KBaRE(BO3)2 (RE = Sm, Eu, Gd, Tb, Dy, Ho, Er, Tm, Yb, Lu) series: materials with a triangular rare earth lattice 036002
Tuning magnetic properties in quasi-two-dimensional ferromagnetic Fe2-xAs2Te2 (0 ≤ x ≤ 0.85) 036003
Magnetic and dielectric properties of Cu-Co substituted BiFeO3 multiferroics 036004

Photonic materials

- The mechanical, electronic and optical properties of KH under high pressure: a density functional theory study 036001
Influence of bis-thiourea nickel nitrate on the structural, optical, electrical, thermal and mechanical behavior of a KDP single crystal for NLO applications 036002
Enhancement of below gap photoluminescence of InAs single crystal via suppression of native defects 036003
Substitution mechanisms and location of Co2+ ions in congruent and stoichiometric lithium niobate crystals derived from electron paramagnetic resonance data 036004
Sol-gel synthesis and photoluminescence of SiO2-SiEr3+ nanocomposite films 036005

Electronic materials

- The conventional cell and the primitive cell electronic structure of anatase titanium dioxide crystal 036001
Structural, electronic and optical properties of BeTi2: A density functional theory study 036002
Electronic reconstruction of hexagonal FeS: a view from density functional dynamical mean-field theory 036003
Effects of amount of graphene oxide and the times of LightScribe on the performance of all-solid-state flexible graphene based micro-supercapacitors 036004

Alternative technological development for RF hybridization

- Synthetic effect of PEG and hydrosol treatments of solution on preparing Al2O3 coating by cathode plasma electrolytic deposition 036006

Thin films

- Effect of doping on the surface modification of nebulizer sprayed Ba2Zn1-xO nanocrystalline thin films 036001
Role of oxygen pressure on the structural, morphological and optical properties of c-Al2O3 films deposited by enhanced photo catalytic performance of nickel doped bismuth selenide under visible light irradiation 036002
Interactions between Er dopant and intrinsic point defects of ZnO: a first-principles study 036003
Reciprocal space mapping study of CdTe epilayer grown by molecular beam epitaxy on (110) 2B GaAs substrate 036004
Growth of freestanding lead dihalide thin films and microtubule via hydrothermal method 036005
Studies on structural, optical and magnetic properties of cobalt substituted magnetite fluids (CoFe2-xFe2O4) 036006

Direct fabrication of CIGS electrode target and room temperature deposition of thin films with low work function

- Wenwei Zou, Karim Khan, Xunna Zhao, Changzhou Zhu, Jinhua Huang, Jie Li, Ye Yang and Weijie Song 036003

Metals and alloys

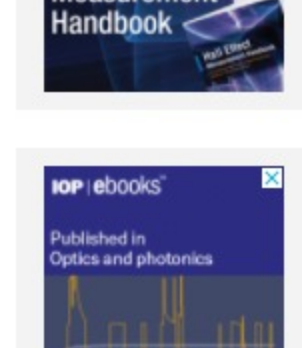
- Effect of friction stir welding on microstructure and corrosion behavior of LFe aluminum alloy 036001
Explosive compact-coating of tungsten-copper alloy on a copper surface 036002

Corrigendum

- FREE ARTICLE
Corrigendum: Tunability of morphological properties of Nd-doped TiO2 thin films (Mater. Res. Express 3 (2016) 033503) 036001

JOURNAL LINKS

- Submit an article
About the journal
Editorial board
Author guidelines
Review for this journal
Publication charges
News and editorial
Awards
Journal collections
Pricing and ordering
Contact us





Materials Research Express

Editorial Board

Anna Balazs University of Pittsburgh, Pittsburgh, PA, USA

Sarbajit Banerjee Texas A&M University, College Station, TX, USA

Michael Bevan Johns Hopkins University, Baltimore, MD, USA

Liming Dai Case Western Reserve University, Cleveland, OH, USA

Israel Felner The Hebrew University of Jerusalem, Jerusalem, Israel

Claudia Felser Johannes Gutenberg University of Mainz, Mainz, Germany

Jacek Kossut Polish Academy of Sciences, Warsaw, Poland

Dimitrios Maroudas University of Massachusetts, Amherst, MA, USA

Tony McNally University of Warwick, UK

C N R Rao Jawaharlal Nehru Centre for Advanced Scientific Research, Bangalore, India

R Riggelman University of Pennsylvania, Pennsylvania, PA, USA

D D Sarma Indian Institute of Science, Bangalore, India

Sabyasachi Sen University of California, Davis, CA, USA

Prashant Sonar Queensland University of Technology, Australia

Zhiyong Tang National Center for Nanoscience and Technology, China

Xiaobo Yin University of Colorado, Boulder, CO, USA

Materials Research Express also has an [Advisory Board](#).

JOURNAL LINKS

[Submit an article](#)

[About the journal](#)

[Editorial Board](#)

[Author guidelines](#)

[Review for this journal](#)

[Publication charges](#)

[News and editorial](#)

[Awards](#)

[Journal collections](#)

[Pricing and ordering](#)

[Contact us](#)

PAPER

Synthesis and characterization of carbon nanoparticle/PVA/ chitosan for security ink applications

To cite this article: B W Nuryadin *et al* 2017 *Mater. Res. Express* **4** 034003

View the [article online](#) for updates and enhancements.

Related content

- [A simple strategy for synthesizing highly luminescent carbon nanodots and application as effective down-shifting layers](#)
Xugen Han, Sihua Zhong, Wei Pan et al.
- [Sintering time optimization on red photoluminescence properties of manganese-doped boron carbon oxynitride \(BCNO:Mn\) phosphor](#)
Bebeh Wahid Nuryadin, Yayu Suryani, Yuli Yuliani et al.
- [Carbon dots-decorated TiO₂ nanotubes arrays used for photo/voltage-induced organic pollutants degradation and inactivation of bacteria](#)
Lingyan Feng, Hanjun Sun, Jinsong Ren et al.



PAPER

Synthesis and characterization of carbon nanoparticle/PVA/chitosan for security ink applications

RECEIVED
13 November 2016REVISED
4 February 2017ACCEPTED FOR PUBLICATION
14 February 2017PUBLISHED
10 March 2017B W Nuryadin^{1,2}, R Nurjanah^{1,2}, E C S Mahen^{1,3} and A Y Nuryantini^{1,3}¹ Physics of Nanomaterial Laboratory, UIN Sunan Gunung Djati Bandung, Jalan A.H. Nasution 105, Bandung 40614, Indonesia² Department of Physics, UIN Sunan Gunung Djati Bandung, Jalan A.H. Nasution 105, Bandung 40614, Indonesia³ Department of Physics Education, UIN Sunan Gunung Djati Bandung, Jalan A.H. Nasution 105, Bandung 40614, IndonesiaE-mail: bebehwahid102@uinsgd.ac.id**Keywords:** carbon nanoparticle, security ink application, PVA/chitosan composite**Abstract**

Security ink using a carbon nanoparticle (C-dot)/PVA/chitosan-composite-based material has been successfully synthesized. The C-dot powder was prepared using a urea pyrolysis method. The precursors were synthesized using urea ((NH₂)₂CO, Mw = 60.07 g mol⁻¹) and citric acid (C₆H₈O₇·H₂O, Mw = 210.14 g mol⁻¹) as the fuel and carbon sources, respectively. The C-dots were prepared by heating the precursor solution at 250 °C for 90 min. The security ink was fabricated using C-dots, polyvinyl alcohol (PVA, (CH₂CH(OH))_n, with Mw = ~20 000 g mol⁻¹) and chitosan as the dyes, resins and binders, respectively. The morphology and optical properties of the security ink were measured using SEM and EDX, a PL spectrometer and UV-vis spectroscopy. The viscosity properties of the security ink were measured using a viscometer. The characterization showed that the C-dots have a monodisperse particle size, a tetragonal structure and absorption spectra in the UV light region. It is shown that the PVA:chitosan concentration has a significant effect on the viscosity properties, so the viscosity is optimized for the security ink. In addition, the security ink was studied using a commercial printer, and the results show a good quality blue emission (450 nm) appearing under UV light exposure at 365 nm. The security ink C-dot/PVA/chitosan composite has potential applications in security, panel display, optoelectronic and optical devices on an industrial scale.

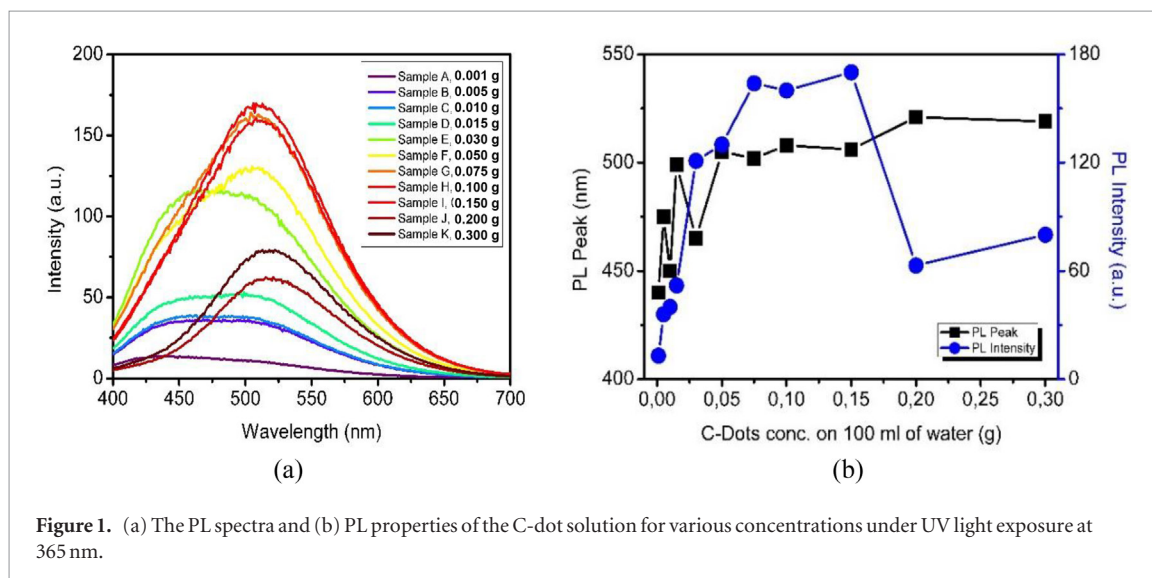
1. Introduction

Luminescent materials have semiconductor-like properties, which change in response to the stimulus of external radiation, such as that from UV light, thermal or nuclear sources. Luminescent materials have optical security features that are difficult to imitate and duplicate. Therefore, they are widely used as non-colour security inks for applications in optical data recording, storage and security [1]. Some photoluminescent materials have been widely used as fluorescent ink in organic dyes [2], conjugated polymers [3] and inorganic quantum nanodots [4]. Organic dye has low photostability and a small Stokes shift, while the conjugated polymers and inorganic quantum nanodots have a fluorescence characteristic that is easily tuneable with a narrow emission bandwidth and high photostability. In recent years, nanoparticles doped by lanthanide atoms and/or rare earth metal ions have been developed for application in anti-counterfeiting security ink. However, there are concerns regarding the long-term cytotoxicity risk and potential environmental pollution caused by lanthanide and rare-earth-ion-based security ink [5].

In recent research, our group succeeded in developing a new type of graphitic carbon-nanoparticle-based C-dot fluorescent material without using rare earth ions [6]. C-dots are the most stable allotropes of carbon, and their potential has developed due to their unique electronic and optical properties [7]. C-dots can be synthesized on a large scale using a nitrogen condensation process, including the use of melamine, urea and thiourea [8]. C-dots have been successfully developed for various applications, such as in solar absorber materials, bioimaging and sensors [9–11]. Compared with inorganic quantum nanoparticles, C-dots have many advantages such as their simple fabrication process, high quantum efficiency, good biocompatibility, low cost and cytotoxicity and high photostability [9].

Table 1. The various PVA and chitosan mass concentrations in 100 ml of distilled water.

Sample	PVA (g)	Chitosan (g)
Non-blend	0	0
Blend 1	0.4	0.1
Blend 2	0.8	0.2
Blend 3	1.6	0.4
Blend 4	2.8	0.7

**Figure 1.** (a) The PL spectra and (b) PL properties of the C-dot solution for various concentrations under UV light exposure at 365 nm.

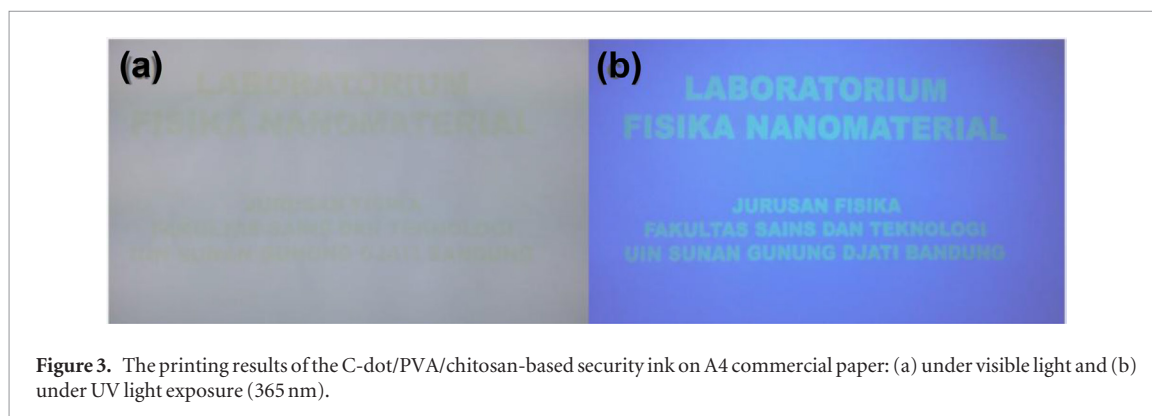
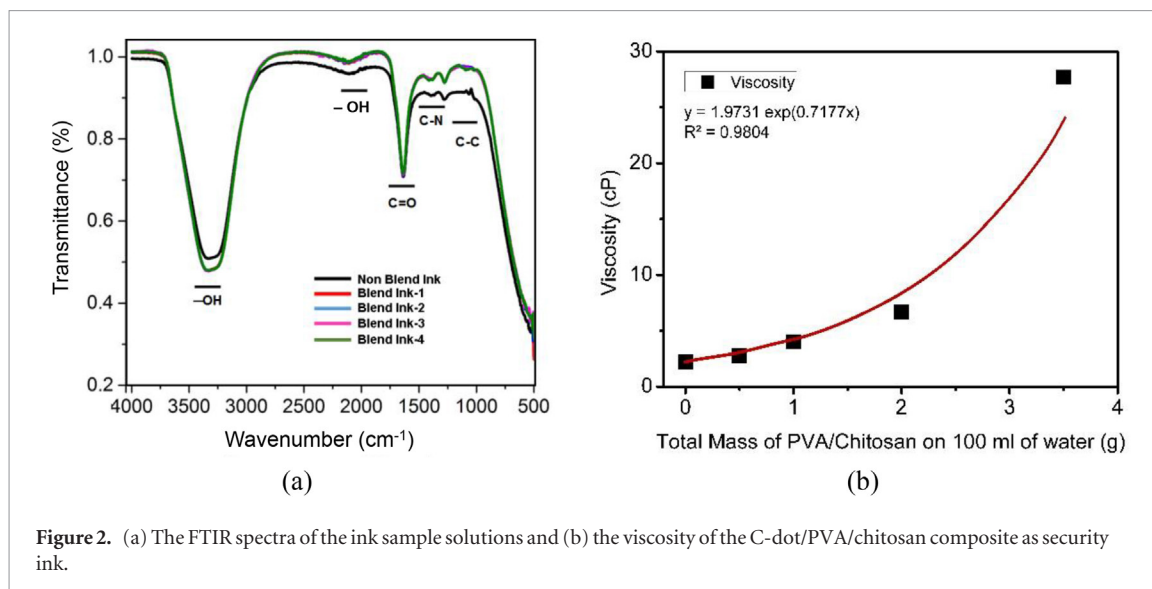
In this paper, we report the synthesis and characterization of a C-dot/PVA/chitosan-composite-based security ink prepared by the wet chemical method. We used PVA and chitosan as adhesives to control the oxidation and dissolution of the C-dot particles after printing. We varied the PVA/chitosan concentration synthesis to determine the composite viscosity optimization of the C-dot/PVA/chitosan-composite-based security ink. The morphology, viscosity and optical properties of the C-dot/PVA/chitosan-composite-based security ink were measured using SEM and EDX, a viscosity meter, a PL spectrometer, and UV-vis spectroscopy.

2. Experiment

The C-dot powder was synthesized using citric acid and urea as the carbon and fuel source, respectively. The precursor solution was prepared by mixing all the raw materials with a carbon/fuel (C/N) mass ratio of 3 g/3 g. The precursors were heated at 250 °C for 90 min using a commercial oven to obtain a black carbon powder [12]. The C-dot solution was prepared by dispersing the synthesized carbon powder with a varying mass from 0.01 g to 0.3 g in 20 ml of pure water. The C-dot solution was stirred using a magnetic stirrer until all the carbon powder had dispersed and become a clear brown solution.

The security ink was fabricated using the prepared C-dots, polyvinyl alcohol (PVA, $M_w = \sim 20\,000\text{ g mol}^{-1}$) and chitosan (β -(1-4)-linked D-glucosamine and N-acetyl-D-glucosamine) to form a colloidal composite of C-dot/PVA/chitosan. The C-dot/PVA/chitosan composite synthesis has several steps: first, the chitosan powder is slowly dissolved in pure water with 2% acetic acid at room temperature until it becomes a homogeneous chitosan solution. Then, polyvinyl alcohol (PVA) and C-dots are mixed into the chitosan solution and stirred at 70 °C. To optimize the viscosity of the security ink, the PVA/chitosan concentration was varied from 0% to 2.8 % w/v, as shown in table 1. PVA and chitosan with a mass ratio of 4:1 were used to produce a composite polymer with the best hydrophobic properties [13]. In addition, the prepared security ink was printed onto several types of commercial paper to determine the nature of its interaction with the C-dot/PVA/chitosan composite.

The photoluminescence (PL) spectra (Cary Eclipse spectrofluorometer, Agilent, Australia) and the FT infrared spectra (FTIR, Bruker Optics, Ettlingen, Germany) were taken, and scanning electron microscopy (SEM, JEOL JCM-6000 Benchtop, Japan) was conducted to characterize the optical properties, chemical bonding and morphology of the prepared samples, respectively. The viscosity measurement of the optimized C-dot/PVA/chitosan-based security ink was conducted using a rotational viscometer TV-20 Tokimec at room temperature.



3. Results and discussion

The C-dot solution was prepared by dispersing the synthesized carbon powder in pure water. Figure 1(a) shows the PL spectra of the C-dot solution for several concentrations between 0.01 g and 0.3 g in 20 ml of pure water. The PL spectra characterization shows that all the prepared samples of C-dot solution have a blue luminescence with a PL peak from 440 nm to 520 nm. Moreover, the blue luminescence properties of the prepared samples were optimized by the increasing the concentration of the C-dot solution, as shown in figure 1(b). At low concentrations, the C-dot solution has a wide range of PL emission peaks, and possibly two PL peaks at 400 nm and 500 nm. The existence of two PL peaks is caused by the interaction between the C-dots and chitosan with an excitation wavelength at 365 nm [13]. The PL properties showed that sample I, with a C-dot concentration at 0.75% w/v has the highest emission intensity. However, the PL intensity of the C-dot solution decreased for sample J (1% w/v) and sample K (1.5% w/v). The PL properties of the prepared samples show that the electronic structure of the C-dot particles remains unchanged, even when the C-dot concentration is enlarged (see figure 1(b)). However, the optimized PL intensity of the C-dot solution was probably caused by the photon-particle interactions between the C-dot particles and the excitation wavelength. The physical models for these phenomena are: (i) when the number of C-dot particles is low, the amount of C-dot particle emission is lower as well. (ii) When the number of C-dot particles increases, the number of C-dot emission photons is higher as well. However, (iii) when the amount of particles is high, some emitted photons are reabsorbed by the carbon particles, forming a nonradiative recombination, and causing the emission intensity to decrease (quenching effect recombination).

To determine the existing functional groups (chemical bonding) of the security inks, the C-dot/PVA/chitosan-prepared samples were characterized using FTIR, as shown in figure 2(a). The FTIR spectra results indicate the existence of several chemical bonds between the C-dots and the polymers, and also show their interaction, such as C-C at 950–1030 cm^{-1} and C-N at 1400–1420 cm^{-1} . In addition, the functional groups of -OH (water combination band) appear at 3250–3420 cm^{-1} and 1655 cm^{-1} ; these results show the surface interaction between the C-dots, polymers and solvents [13]. This indicates that the C-dot particles have the ability to disperse in water, due to their dominant hydrophilic nature [14]. The chemical bond between the PVA and chitosan was expected to form a composite polymer with the C-dots. Furthermore, when the prepared security ink was printed on a

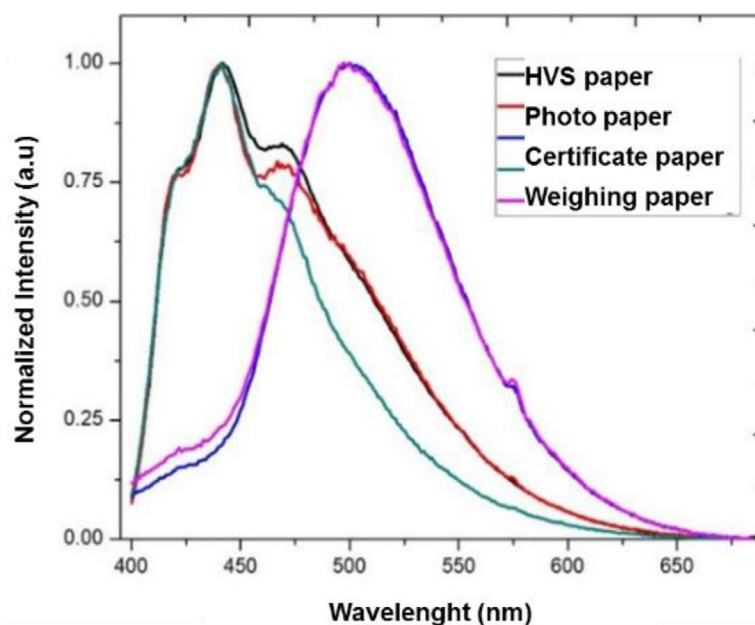


Figure 4. The PL spectra of C-dot/PVA/chitosan printed on various types of paper under UV light exposure at 365 nm.

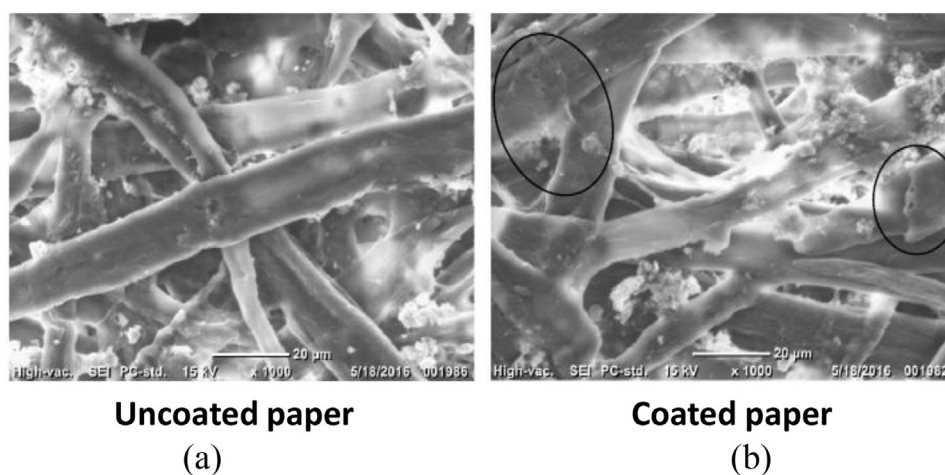


Figure 5. SEM images of the A4 commercial paper (a) uncoated and (b) coated with the C-dot/PVA/chitosan-composite-based security ink.

substrate, such as paper, the PVA/chitosan behaved as a thin layer of composite polymer with strong hydrophobicity. The hydrophobic nature of the PVA/chitosan composite was expected to prevent the re-dissolution or the oxidation process of the C-dot particles. The viscosity of the C-dot/PVA/chitosan composite was measured for various PVA/chitosan concentrations, as shown in figure 2(b). The viscosity results show that the addition of PVA and chitosan increases the viscosity of the security ink exponentially. The increasing viscosity of the C-dot/PVA/chitosan composite might have been caused by the increasing amount of PVA/chitosan bonding crosslinks.

The solution of ink blend 1 was chosen as the security ink for the printing test using a commercial printer (HP Deskjet 1010). The printing stages consisted of: (i) injection of the ink into an empty cartridge, (ii) automatic printing on several types of paper, and (iii) the drying process at room temperature. Figure 3 shows the printing result of the security ink on an A4 paper sample. The initial observation proved that the security ink had successfully been printed on the paper, and exhibited blue emission under UV light exposure (365 nm). To understand the interaction between the security ink and the paper, as well as its influence on the optical properties, the PL spectra were measured for various types of commercial paper. Figure 4 shows the PL spectra of the manually printed prepared security ink on various types of commercial paper. In general, the PL spectra showed that the printed security ink exhibited a blue emission with a PL peak from 410–530 nm under UV light exposure (365 nm). However, the PL spectra showed that the emission properties of the printed results are highly dependent on the interaction of the security ink with the commercial paper. The shift in the properties of the PL was possible, since the paper may

have contained a material that undergoes photoluminescence, such as melamine and others. Therefore, further in-depth study on the interaction between carbon-nanoparticle-based security inks and paper needs to be done.

Figure 5 shows an SEM image of A4 commercial paper both uncoated and coated by the C-dot/PVA/chitosan-composite-based security ink using a commercial printer. The observation results show that the uncoated and coated commercial paper have the same morphological characteristics. On closer inspection, the coated paper had a thin layer of polymer composite on the paper fibres; in addition, the porosity of the coated paper was lower, since the composite polymer had filled in the pores. Therefore, it is concluded that the C-dot/PVA/chitosan-based security ink can be manually or automatically printed, and that the security ink composites strongly interact with the morphology of the paper.

4. Conclusions

Security ink using a carbon nanoparticle C-dot/PVA/chitosan-composite-based material has been successfully synthesized. The C-dot powder was prepared using a urea pyrolysis method. The precursors were synthesized using urea ($(\text{NH}_2)_2\text{CO}$, $M_w = 60.07 \text{ g mol}^{-1}$) and citric acid ($\text{C}_6\text{H}_8\text{O}_7 \cdot \text{H}_2\text{O}$, $M_w = 210.14 \text{ g mol}^{-1}$) as the fuel and carbon sources, respectively. The C-dots were prepared by heating the precursor solution at 250°C for 90 min. The security ink was fabricated using C-dots, polyvinyl alcohol (PVA, $(\text{CH}_2\text{CH}(\text{OH}))_n$, with $M_w = \sim 20\,000 \text{ g mol}^{-1}$) and chitosan as the dyes, resins and binders, respectively. The characterization showed that the C-dots have a monodisperse particle size, a tetragonal structure, and absorption spectra in the UV light region. The viscosity properties show that the PVA:chitosan concentration has a significant effect which optimizes the viscosity of the security ink. In addition, the security ink was studied using a commercial printer, and the printing results show a good quality blue emission (450 nm) appearing under UV light exposure at 365 nm. The C-dot/PVA/chitosan-composite-based security ink has potential applications in security, panel displays, optoelectronic and optical devices on an industrial scale.

Acknowledgments

This work was supported by a research grant (B-200/B2-63/V.2/PP.00.9/06/2016) from UIN Sunan Gunung Djati Bandung, the Ministry of Religious Affairs, the Republic of Indonesia. Author contributions: BWN, RN and AYN contributed to the design, experimental and data processing. AYN, RN and ECSM contributed partly to writing the manuscript draft and BWN completely wrote the manuscript.

References

- [1] Lu Y *et al* 2014 *Nat. Photon.* **8** 32–6
- [2] Hou X, Ke C, Bruns C J, McGonigal P R, Pettman R B and Stoddart J F 2015 *Nat. Commun.* **6** 6884
- [3] Chang K, Liu Z, Chen H, Sheng L, Zhang S X-A, Chiu D T, Yin S, Wu C and Qin W 2014 *Small* **10** 4270–5
- [4] Nasution E L Y, Ahab A, Nuryadin B W, Haryanto F, Arif I and Iskandar F 2016 *AIP Conf. Proc.* **1710** 030007
- [5] Nuryadin B W, Mahen E C S, Iskandar F, Ogi T, Okuyama K, Abdullah M and Khairurrijal E 2014 *Adv. Mater. Res.* **896** 464–7
- [6] Chen X, Jin Q, Wu L, Tung C and Tang X 2014 *Angew. Chem., Int. Ed.* **53** 12542–7
- [7] Wang X, Maeda K, Thomas A, Takanabe K, Xin G, Carlsson J M, Domen K and Antonietti M 2009 *Nat. Mater.* **8** 76–80
- [8] Wang Y, Wang X and Antonietti M 2012 *Angew. Chem., Int. Ed.* **51** 68–89
- [9] Baker S N and Baker G A 2010 *Angew. Chem., Int. Ed.* **49** 6726–44
- [10] Ray S C, Saha A, Jana N R and Sarkar R 2009 *J. Phy. Chem. C* **113** 8546–51
- [11] Zhang P, Li W, Zhai X, Liu C, Dai L and Liu W 2012 *Chem. Commun.* **48** 10431–3
- [12] Mahen E C S, Nuryadin B W, Iskandar F, Abdullah M and Khairurrijal E 2015 *AIP Conf. Proc.* **1586** 136–8
- [13] Pan X, Ren W, Gu L, Wang G and Liu Y 2014 *Aust. J. Chem.* **67** 1422–6
- [14] Lee D W, Lim C, Israelachvili J N and Hwang D S 2013 *Langmuir* **29** 14222–9